Polymer Chemistry

Tunable Polyethylene-polypropylene Blends via Compatibilization through Nitrene Insertion-Enabled Dynamic Covalent Crosslinking

Journal:	*Polymer Chemistry*
Manuscript ID	PY-ART-11-2024-001355.R1
Article Type:	Paper
Date Submitted by the Author:	30-Jan-2025
Complete List of Authors:	Shrestha, Roman; University of California, Chemistry Guan, Zhibin; University of California, Chemistry

ARTICLE

Tunable Polyethylene-polypropylene Blends via Compatibilization through Nitrene Insertion-Enabled Dynamic Covalent Crosslinking

Received 00th January 20xx,
Accepted 00th January 20xx

DOI: 10.1039/x0xx00000x

Roman Shrestha,[a] and Zhibin Guan*[a,b,c]

Polymer blends offer a cost-effective way to create new materials with enhanced properties. However, blending different polymers often results in phase separation with weak interfacial adhesion, leading to inferior mechanical properties. Given that high-density polyethylene (HDPE) and isotactic polypropylene (iPP) are the largest volume polymers, there is significant interest in developing blends of these materials. Applying a singlet nitrene-facilitated dynamic crosslinking method recently developed in our lab, in this study we prepared a series of HDPE/iPP blends across a range of compositions with enhanced compatibility and tunable thermomechanical properties. By incorporating a small amount of a dynamic crosslinker featuring a siloxane core and bis-aromatic sulfonyl azides (bis-ASA) into varying compositions of HDPE and iPP, we achieve significant improvements in the compatibility. AFM and SEM imaging analyses reveal that the compatibilized blends exhibit superior homogeneity compared to control blends. Additionally, these blends show significant improvements in elongation at break, toughness, and oxidative stability. The dynamic crosslinking further enhances the blends' creep resistance while retains reprocessability, paving the way for the development of tailorable polymer blends for various applications.

Introduction

Polymer blends are physical mixtures of two or more different polymers that are combined to produce a material with enhanced or tailored properties.[1] Polymer blending provides an attractive low-cost approach to accessing new materials without the need of synthesizing new polymers.[1] The inclusion of multiple polymers in blends can enhance the overall properties by combining the distinct characteristics of each individual polymer. Furthermore, the properties of blends can be tuned by varying the composition of the blends.

Polymer blends can be classified into three types based on the interactions between the polymers: miscible, immiscible, and compatible blends.[2] Miscible polymer blends exhibit homogeneous mixing at the molecular level and show a single glass transition temperature (T_g) following the Flory-Fox equation.[3] In contrast, immiscible polymer blends show heterogeneous phase behavior and retain the T_g's of the component polymers. Blending immiscible polymers often results in macroscopic phase separation with weak interfacial adhesion, leading to low-stress transfer and brittle materials.[2] To address this, immiscible blends are often compatibilized to reduce phase separation and achieve a finely dispersed phase morphology. This improves their physical and mechanical properties by enhancing interfacial adhesion between the components.

Traditional compatibilization techniques can generally be divided into two main categories: nonreactive and reactive compatibilization. Nonreactive compatibilization uses pre-made compatibilizers such as block copolymers[4-8], graft copolymers[9-12], and random copolymers[13]. These compatibilizers reduce interfacial tension and droplet size to achieve a fine morphology in the blends. Reactive compatibilization, on the other hand, involves in situ chemical reactions between functional groups of the component polymers during blending.[14-16] This forms covalent connections between different polymers at the interfaces, reducing phase separation and improving the mechanical properties of the polymer blends.[14] However, these designer compatibilization methods must be tailored to varying blend compositions of different polymers.

Recently our lab[17] and Clarke et al.[18] independently introduced a novel strategy using dynamic covalent crosslinking for general polymer compatibilization. In our design, when a bis-aromatic sulfonyl azide (bis-ASA) dynamic crosslinker is heated during polymer blending, it forms reactive singlet aromatic sulfonyl nitrene in situ that can efficiently cross-link different polymers through C-H insertions. Additionally, we have shown that the fluoride-catalyzed dynamic siloxane motif in the dynamic crosslinks enables reprocessability and recyclability of polymer blends.[19]

Our previous study was mainly focused on developing a general compatibilization strategy for facilitating the recycling of mixed plastic waste.[17] In the current study, we demonstrate that our nitrene-enabled dynamic crosslinking method can be used to improve the compatibility and create tunable HDPE/iPP blends across a range of compositions (Figure 1). Polyethylene (PE) and polypropylene (PP) are among the most widely manufactured plastics in the world, accounting for 184 million

[a] Department of Chemistry, University of California, Irvine, California, 92697, United States
[b] Department of Materials Science and Engineering, University of California, Irvine, California, 92697, United States
[c] Department of Biomedical Engineering, University of California, Irvine, California, 92697, United States
Supplementary Information available: [details of any supplementary information available should be included here]. See DOI: 10.1039/x0xx00000x

metric tons each year.[20-21] Given their high-volume production and low cost, there is significant interest in developing HDPE/iPP blends. However, due to their immiscible nature, HDPE/iPP blends must be compatibilized for achieving useful mechanical properties. Several reactive[14-16] and non-reactive compatibilization[4-13] approaches have been reported to compatibilize immiscible HDPE/iPP blends but still lack an efficient and general method that could easily tune their mechanical properties for potential large-scale applications. In this study, we achieve the compatibilization of HDPE/iPP by introducing a relatively small quantity of dynamic crosslinks during reactive extrusion (Figure 1). A series of HDPE/iPP blends were prepared and their thermomechanical properties were investigated. Phase imaging analyses by AFM and SEM show that compatibilized blends are more homogeneous than control blends. Furthermore, dynamic crosslinking improves the toughness and creep resistance of the HDPE/iPP blends while maintaining reprocessability, offering tailorable polymer blends for potential applications.

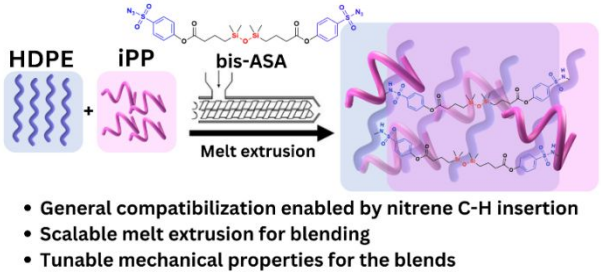

Fig. 1 Schematic illustration of dynamic covalent crosslinking via bis-ASA siloxane crosslinker through reactive extrusion for compatibilization of HDPE/iPP blends with tunable thermomechanical properties.

Experimental

Materials

Sodium 4-hydroxybenzenesulfonate dihydrate (98%, Sigma-Aldrich), oxalyl chloride (98%, TCI America), N,N-dimethylformamide (DMF, ACS grade, Macron Fine Chemicals), sodium azide (99%, Fisher Scientific), 1-(3-dimethylaminopropyl)-3-ethylcarbodiimide hydrochloride (EDC•HCl, Advanced Chemtech), 4-dimethylaminopyridine (DMAP, 99%, Alfa Aesar), 1,3-bis(3-carboxypropyl)tetramethyldisiloxane (97%, Aaron Chemicals), tetrabutylammonium fluoride trihydrate (TBAF, 98%, Oakwood Chemical), dibenzo-18-crown-6 (99%, TCI America), and potassium fluoride (99%, Sigma-Aldrich) were used without further purification. High-density polyethylene (HDPE, MFI = 2.2 g/10 min at 190 °C with a 2.16 kg load, Sigma-Aldrich) and isotactic polypropylene (iPP, Mw = 340,000 g/mol, Mn = 97,000, MFI = 4 g/10 min at 230 °C with a 2.16 kg load, Sigma-Aldrich) were milled into a fine powder with a Fritsch Pulverisette rotary mill fitted with a 0.5 mm sieve cassette. The commercially purchased solvents were used as is.

Synthesis of bis-aromatic sulfonyl azide (bis-ASA) siloxane crosslinker

The bis-ASA siloxane dynamic crosslinker was synthesized in two steps by following our previous report.[17]

bis-ASA siloxane crosslinker. ^{1}H NMR (500 MHz, $CDCl_3$, 298 K) δ 7.99 – 7.97 (m, 4H), 7.35 – 7.34 (m, 4H), 2.63 (t, J = 7.3 Hz, 4H), 1.81 – 1.78 (m, 4H), 0.67 – 0.63 (m, 4H), 0.11 (s, 12H).
^{13}C NMR (151 MHz, $CDCl_3$, 298 K) δ 171.01, 155.57, 135.44, 129.27, 122.97, 37.52, 18.95, 17.92, 0.30.
TOF-MS ESI calcd. for $C_{24}H_{32}N_6O_9S_2Si_2$, $[M+Na]^+$ = 691.1108 m/z, found 691.1133 m/z.

Atomic Force Microscopy (AFM) Imaging

The morphology of control and compatibilized blends were imaged using Oxford Instruments Asylum Research MFP-3D in AC mode. The tensile heads from compressed samples were cryo-microtomed at –140 °C using a Leica EM UC7 Ultramicrotome. Smooth cutting surfaces were obtained using a glass knife, and 500 nm flat slices were obtained via cutting at a speed of 0.4 mm/min. The 500 nm slices were directly mounted on a drop of DI water on a clean silicon wafer taped to a glass plate. AFM was operated in the repulsive regime with silicon cantilevers AC240TS-R3 with resonance frequency of 70 kHz and spring constant of 2 N/m.

Scanning Electron Microscopy (SEM) Imaging

The tensile heads were equilibrated under the temperature of liquid nitrogen and cryo-fractured using pliers. The cryo-fractured samples were coated with Ir (5-7 nm) using EMS 150T Sputter Coater. SEM was performed on FEI Magellan 400 XHR with an accelerating voltage of 5-15 kV.

Compression moulding and uniaxial tensile testing

The extrudates were compression-moulded on stainless steel moulds into dumbbell shapes (ISO 527-2 type 5B) and cooled using water circulation (400 mL/min). The moulded samples were trimmed and cut with an X-ACTO knife for tensile testing. The tensile samples were tested on an Instron 3365 mechanical tester fitted with pneumatic grips at a crosshead velocity of 10 mm/min.

Results and Discussion

A series of HDPE/iPP blends with varying compositions (70/30, 50/50, and 30/70) and crosslinker loadings (0.5, 1, 2 wt%) were prepared on a twin-screw extruder at 190 °C for 8 minutes at 130 rpm, both with and without the addition of the bis-ASA dynamic crosslinker plus fluoride catalyst. Our previous study has shown that the in-situ generated singlet nitrene exhibits the highest reactivity for C-H insertion toward tertiary C-H bonds, with significantly lower reactivity observed for secondary and primary C-H bonds.[17] The abundance of tertiary C-H bonds in iPP makes it more reactive towards the singlet nitrene, so for blends with a higher proportion of iPP, less bis-ASA crosslinker was used to avoid over crosslinking. Based on this consideration and optimization, we first prepared a series of HDPE/iPP blends at 70/30, 50/50, and 30/70 compositions with 2, 1, and 0.5 wt% loadings of bis-ASA dynamic crosslinker, respectively. For the 30/70 HDPE/iPP system, 1 wt% crosslinker loading obtained the blend with 25% gelation, while the same crosslinker loading for the 50/50 HDPE/iPP blend showed 23% gelation. This is in agreement that higher iPP concentrations in the HDPE/iPP blend achieve more crosslinking with the same amount of bis-ASA crosslinker addition. For the 70/30 HDPE/iPP blend, higher level of the bis-ASA crosslinker (2 wt%) was added in order to

form comparable cross-links (Table S3, Supporting Information).

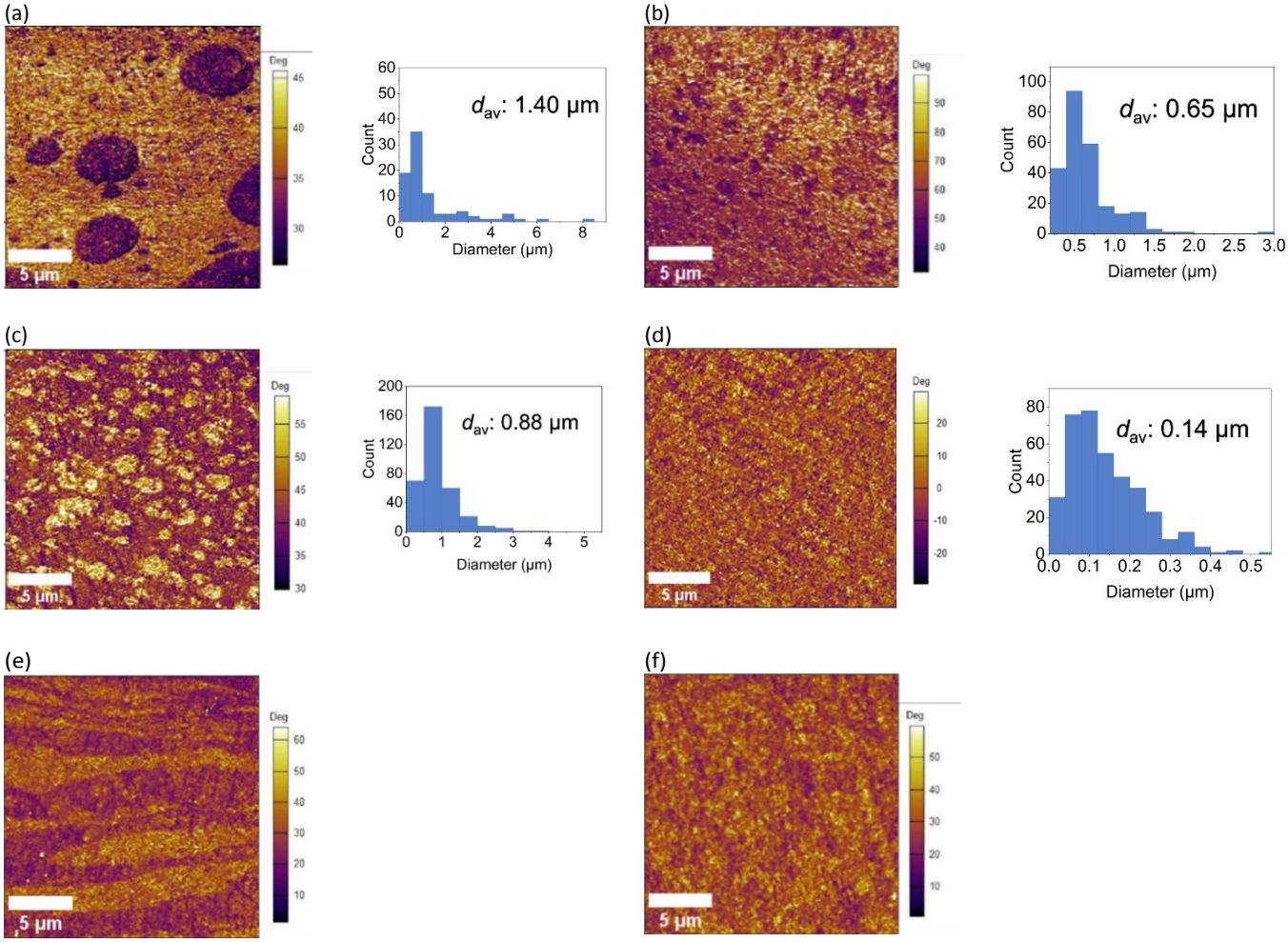

Fig. 2 AFM phase images of the 70/30 HDPE/iPP control (a) and with 2 wt% bis-ASA crosslinker (b); 30/70 HDPE/iPP control (c) and with 0.5 wt% bis-ASA crosslinker (d); 50/50 HDPE/iPP control (e) and with 1 wt% bis-ASA crosslinker (f).

To verify the crosslinking was indeed mediated by the bis-ASA dynamic crosslinker, the compatibilized HDPE/iPP blends were shown to fully dissolve in mesitylene upon the addition of excess tetrabutylammonium fluoride (TBAF), confirming that all crosslinks in the networks are due to the siloxane-containing bis-ASA crosslinker (Section 4.3, Supporting Information). The dissolution of the dynamically crosslinked blends with excess TBAF was due to the high affinity of F^- towards silicon and the formation of a stable Si-F bond breaking the crosslinking bonds.

The extruded control and compatibilized blends were moulded at 200 °C for 10 minutes, followed by a hot press at 160 °C for 15 minutes to obtain sample specimens for further tests. Cryo-microtomed samples were subjected to atomic force microscopy (AFM) imaging analysis of the microphase morphology (Figure 2). The AFM images of the control blends show phase-separated morphology with an average droplet size of 1.40 mm for 70/30 HDPE/iPP blend and 0.88 mm for 30/70 HDPE/iPP blend, which is close to the reported literature for these blend systems.[23] The compatibilized blends exhibit better homogeneity in their morphology with the reduction in droplet size from 1.40 mm to 0.65 mm for 70/30 HDPE/iPP blend (Figure 1a,b), and from 0.88 mm to 0.14 mm for 30/70 HDPE/iPP blends (Figure 1c,d), respectively. For the 50/50 HDPE/iPP blend, while the control blend shows co-continuous morphology[24,25], the dynamically crosslinked blend exhibits much more homogeneous morphology.

To further confirm the phase morphology, the cryo-fractured surfaces of the control and compatibilized blends were observed using scanning electron microscopy (SEM). The SEM images (Figure 3a-d) showed larger domain features in the 70/30 and 30/70 HDPE/iPP control blends compared to the compatibilized blends, which is consistent with the AFM images. The SEM images of the compatibilized 50/50 HDPE/iPP blend show more homogeneous morphology in contrast to the co-continuous morphology of its control blend (Figure 3e-f). Both AFM and SEM images confirm that our dynamic crosslinking chemistry facilitated by the in situ generated single nitrene was effective for the compatibilization of immiscible HDPE/iPP blends.

After confirming the compatibilization of immiscible HDPE/iPP blends, their thermomechanical properties were investigated to show that the introduction of dynamic crosslinks enhances their properties. The mechanical properties of the compatibilized blends were compared to their respective control blends through tensile testing. Due to the immiscibility and large phase separation, all HDPE/iPP control blends are

brittle with relatively low elongation at break, which aligns with previous studies.[4,6,23]

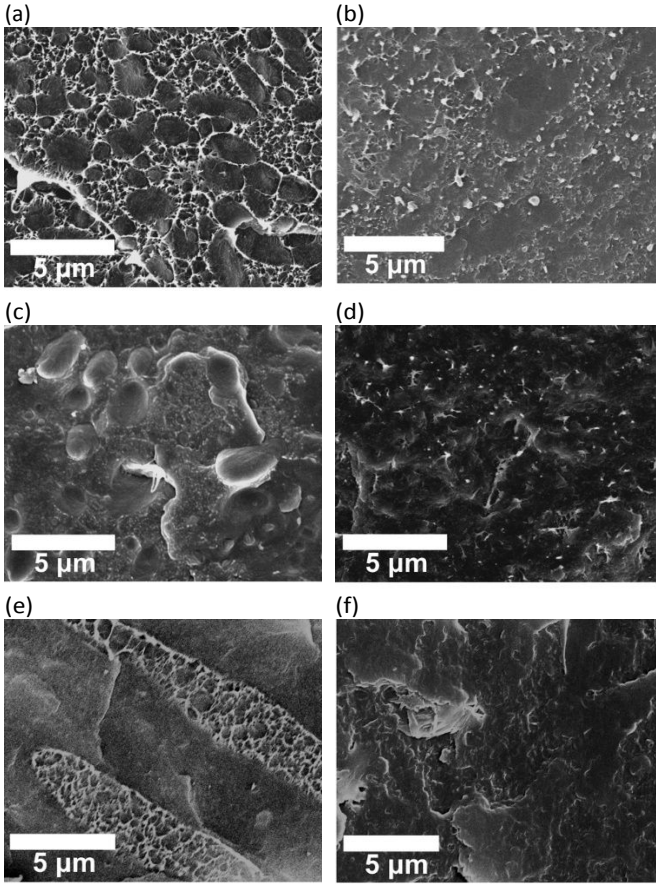

Fig. 3 SEM images of the 70/30 HDPE/iPP control (a) and with 2 wt% bis-ASA crosslinker (b); 30/70 HDPE/iPP control (c) and with 0.5 wt% bis-ASA crosslinker (d); 50/50 HDPE/iPP control (e) and with 1 wt% bis-ASA crosslinker (f).

The addition of 2 wt% bis-ASA crosslinker improved the elongation at break for the 70/30 HDPE/iPP blend from 25% to approximately 70% (Figure 4a). The compatibilized 70/30 HDPE/iPP blend exhibited a 164% increase in toughness compared to the control blend. Similarly, the addition of 0.5 wt% bis-ASA crosslinker for the 30/70 HDPE/iPP and 1 wt% bis-ASA crosslinker for the 50/50 HDPE/iPP blends enhanced the elongation at break from 9% to 41% (Figure 4a). Similarly, the compatibilized 30/70 HDPE/iPP blend showed a 495% increase in toughness, while the compatibilized 50/50 HDPE/iPP blend demonstrated a 511% increase. These results correlate well with the morphologies observed with AFM and SEM images, demonstrating that the compatibilization by the dynamic crosslinking contributes to the improved mechanical performance. In contrast to the significant improvement in elongation at break, the change in tensile strength is relatively modest. This may be attributed to a decrease in crystallinity caused by crosslinking (Figure S4), which could counteract any potential increase in tensile strength resulting from the crosslinking process, leading to no substantial overall change in tensile strength.

In addition to tuning the properties through changing the ratio of HDPE/iPP, the mechanical properties can also be controlled by varying the loading of the bis-ASA dynamic crosslinkers (0.5, 1, and 2 wt%) at a fixed HDPE/iPP composition of 30/70. At 0.5 wt% crosslinker loading, we did

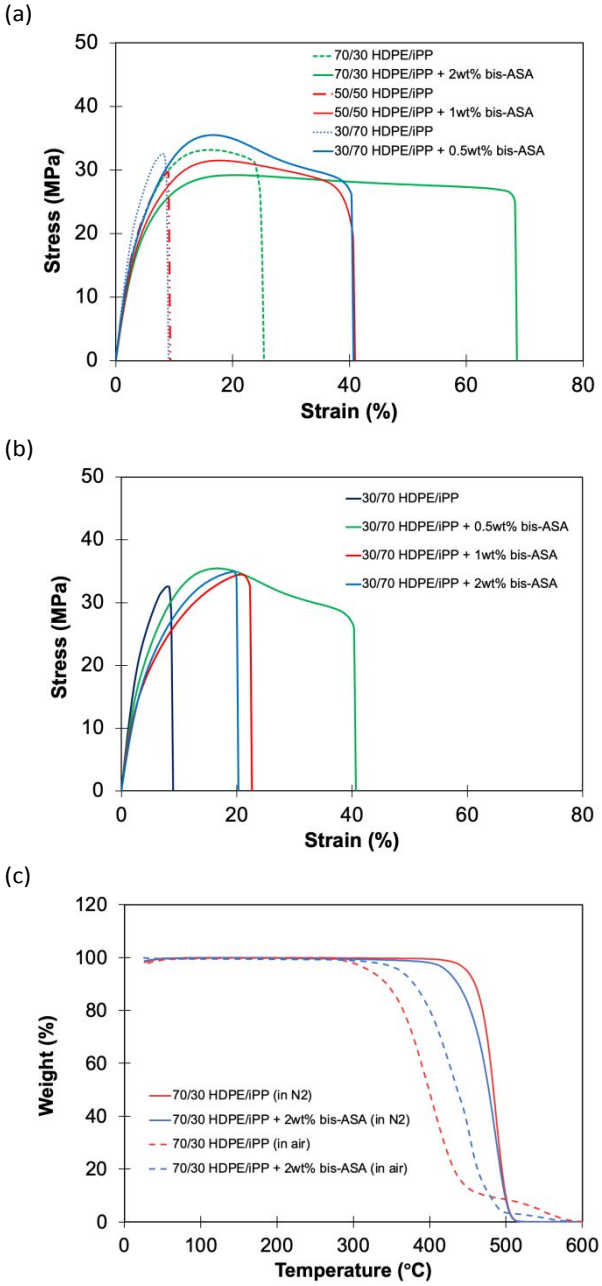

Fig. 4 (a) Uniaxial tensile stress-strain curves for 70/30, 50/50, and 30/70 HDPE/iPP system; (b) Uniaxial tensile stress-strain curves for 30/70 HDPE/iPP with 0.5 wt%, 1 wt%, and 2 wt% crosslinker loading; (c) TGA studies of 70/30 HDPE/iPP system under nitrogen and air atmosphere.

not observe any gelation from the gel fraction assay (Table S3, Supporting Information), suggesting the formation of branched copolymers that help compatibilize the blend with increased elongation at a break (Figure 4b). In contrast, the addition of 1 wt% crosslinker showed 25% gelation and 2 wt% crosslinker showed 27% gelation (Table S3, Supporting Information), with reduced elongation at break for both samples (Figure 4b). The increased crosslinking networks make HDPE/iPP blends more rigid and harder to elongate.

Differential scanning calorimetry (DSC) shows the decrease of crystallinity for both HDPE and iPP for the compatibilized blends compared to the control (Figure S4, Supporting Information), in agreement with earlier observations that the introduction of crosslinks decreases the crystallinity.[17,22] Thermogravimetric analysis (TGA) was used to assess the thermal stability of the compatibilized 70/30 HDPE/iPP blend compared to the control blend. Under an inert atmosphere of nitrogen, they exhibited negligible differences (Figure 4c). However, under the atmosphere of regular air, the compatibilized blend showed improved oxidative stability (Figure 4c), consistent with our earlier observations.[17]

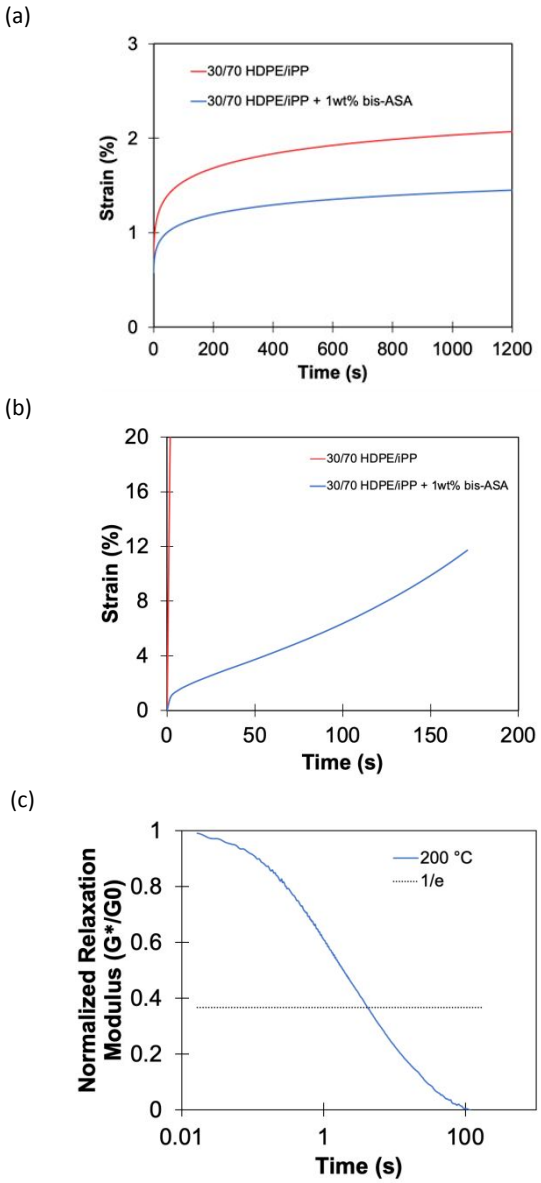

Fig. 5 (a) Creep test of 30/70 HDPE/iPP system at 80 °C under a stress of 2000 Pa; (b) Creep test of 30/70 HDPE/iPP system at 200 °C under a stress of 500 Pa; and (c) Stress relaxation of 30/70 HDPE/iPP + 1 wt% bis-ASA at 200 °C.

We previously reported that introducing dynamic crosslinks to homopolymers resulted in significant improvement of creep resistance of the polymer.[11] Here we observed the same trend for HDPE/iPP polymer blends by testing creep resistance at two conditions. Under high stress of 2 kPa, at a working temperature of 80 °C, the compatibilized 30/70 HDPE/iPP blend with 1 wt% dynamic crosslinker has significantly improved creep resistance than the control blend (Figure 5a). At 200 °C, the 30/70 HPDE/iPP control blend flows like a liquid, unlike the compatibilized blend which creeps much slowly even at such a high temperature (Figure 5b). This enhanced creep resistance property is attributed to the dynamic crosslinks introduced to the blends. Importantly, the dynamic crosslinking enables reconfiguration of the network topology, allowing the compatibilized blends to achieve flow-state reprocessing at elevated temperatures. This was demonstrated by stress-relaxation of the blends at elevated temperatures (Figure 5c).

Conclusions

Using a singlet nitrene-based dynamic crosslinking method recently developed in our lab, in this study we created a series of HDPE/iPP blends with varying compositions that demonstrate improved compatibility and tunable thermomechanical properties. By introducing a small amount of a dynamic crosslinker containing a siloxane core and bis-ASA into different HDPE/iPP blends, we achieved marked enhancements in compatibility. AFM and SEM imaging reveal that these compatibilized blends are significantly more homogeneous than control blends. Furthermore, the modified blends exhibit significant improvements in elongation at break, toughness, and oxidative stability. The dynamic crosslinking also increases creep resistance while maintaining reprocessability, opening up possibilities for tailored polymer blends.

Author contributions

Z.G. conceived the project and R.S. carried out all the experimental studies. Both authors analysed the data and wrote the manuscript.

Conflicts of interest

There are no conflicts to declare.

Data availability

The data supporting this article have been included as part of the ESI.†

Acknowledgements

The work was supported by the National Science Foundation under Grant No. DMR-2414685. The authors thank the facilities and instrumentation at the UC Irvine Materials Research Institute (IMRI) which is supported in part by the National Science Foundation through the UC Irvine Materials Research Science and Engineering Center (DMR-2011967). The authors thank Dr. Jordan Castro for his valuable input and assistance with the study; Gabriela Diaz Gorbea at the University of Minnesota for her assistance with the AFM sample preparation method; and James Pedroarena and Kosuke Yokoyama for their help with SEM sample preparation and imaging.

References

1 M. Rubinstein and R. H. Colby, in *Polymer Physics*, eds. M. Rubinstein and R. H. Colby, Oxford University Press, 2003.
2 L. A. Utracki, in *Polymer Blends Handbook*, eds. L.A. Utracki, C.A. Wilkie, Springer Netherlands, Dordrecht, 2014, pp. 1559–1732.
3 C. Koning, M. Van Duin, C. Pagnoulle and R. Jerome, *Progress in Polymer Science*, 1998, **23**, 707–757.
4 J. M. Eagan, J. Xu, R. Di Girolamo, C. M. Thurber, C. W. Macosko, A. M. LaPointe, F. S. Bates and G. W. Coates, *Science*, 2017, **355**, 814–816.
5 Y. Xu, C. M. Thurber, C. W. Macosko, T. P. Lodge and M. A. Hillmyer, *Ind. Eng. Chem. Res.*, 2014, **53**, 4718–4725.
6 J. Xu, J. M. Eagan, S.-S. Kim, S. Pan, B. Lee, K. Klimovica, K. Jin, T.-W. Lin, M. J. Howard, C. J. Ellison, A. M. LaPointe, G. W. Coates and F. S. Bates, *Macromolecules*, 2018, **51**, 8585–8596.
7 Y. Wang and M. A. Hillmyer, Journal of Polymer Science Part A: Polymer Chemistry, 2001, **39**, 2755–2766.
8 C. W. Macosko, P. Guégan, A. K. Khandpur, A. Nakayama, P. Marechal and T. Inoue, *Macromolecules*, 1996, **29**, 5590–5598.
9 A. H. Tsou, C. R. López-Barrón, P. Jiang, D. J. Crowther and Y. Zeng, *Polymer*, 2016, **104**, 72–82.
10 K. Klimovica, S. Pan, T.-W. Lin, X. Peng, C. J. Ellison, A. M. LaPointe, F. S. Bates and G. W. Coates, *ACS Macro Lett.*, 2020, **9**, 1161–1166.
11 C. R. López-Barrón and A. H. Tsou, *Macromolecules*, 2017, **50**, 2986–2995.
12 C.-L. Zhang, L.-F. Feng, X.-P. Gu, S. Hoppe and G.-H. Hu, *Polymer*, 2007, **48**, 5940–5949.
13 M. S. Lee, T. P. Lodge and C. W. Macosko, *Journal of Polymer Science Part B: Polymer Physics*, 1997, **35**, 2835–2842.
14 M. Xanthos and S. S. Dagli, *Polymer Engineering & Science*, 1991, **31**, 929–935.
15 C. Tselios, D. Bikiaris, V. Maslis and C. Panayiotou, *Polymer*, 1998, **39**, 6807–6817.
16 Y. Pietrasanta, J.-J. Robin, N. Torres and B. Boutevin, *Macromolecular Chemistry and Physics*, 1999, **200**, 142–149.
17 J. Castro, X. Westworth, R. Shrestha, K. Yokoyama and Z. Guan, *Advanced Materials*, 2024, **36**, 2406203.
18 R. W. Clarke, T. Sandmeier, K. A. Franklin, D. Reich, X. Zhang, N. Vengallur, T. K. Patra, R. J. Tannenbaum, S. Adhikari, S. K. Kumar, T. Rovis and E. Y.-X. Chen, *Nature*, 2023, **616**, 731–739.
19 C. Tretbar, J. Castro, K. Yokoyama and Z. Guan, *Advanced Materials*, 2023, **35**, 2303280.
20 US EPA, Advancing sustainable materials management: 2018 fact sheet (2018)
21 R. Geyer, J. R. Jambeck and K. L. Law, *Science Advances*, 2017, **3**, e1700782.
22 M. Röttger, T. Domenech, R. van der Weegen, A. Breuillac, R. Nicolaÿ and L. Leibler, *Science*, 2017, **356**, 62–65.
23 L. Shen, G. D. Gorbea, E. Danielson, S. Cui, C. J. Ellison and F. S. Bates, *Proceedings of the National Academy of Sciences*, 2023, **120**, e2301352120.
24 S. Jose, A. S. Aprem, B. Francis, M. C. Chandy, P. Werner, V. Alstaedt and S. Thomas, *European Polymer Journal*, 2004, **40**, 2105–2115.
25 J. Liu and Y. Li, *J Polym Res*, 2024, **31**, 161.

Data availability statement:

The data supporting this article have been included as part of the Supplementary Information.